Stem-like Human Breast Cancer Cells Initiate Vasculogenic Mimicry on Matrigel

Yuki Izawa[1], Karin Kashii-Magaribuchi[1], Kana Yoshida[2], Mayu Nosaka[2], Nanami Tsuji[2], Ai Yamamoto[2], Kana Kuroyanagi[2], Kanoko Tono[2], Misato Tanihata[2], Moe Imanishi[2], Momoka Onishi[2], Mayu Sakiyama[2], Sana Inoue[2] and Rei Takahashi[1,2]

[1]Graduate School of Pharmaceutical Sciences, Doshisha Women's College of Liberal Arts and [2]Faculty of Pharmaceutical Sciences, Doshisha Women's College of Liberal Arts, 97–1 Kodo, Kyotanabe, Kyoto 610–0395, Japan

Vasculogenic mimicry (VM), referring to vasculogenic structures lined by tumor cells, can be distinguished from angiogenesis, and is responsible for the aggressiveness and metastatic potential of tumors. HCC1937/p53 cells were derived from triple-negative breast cancer (TNBC), and used to investigate the roles of breast cancer stem cells (CSCs) in the formation of VM. HCC1937/p53 cells formed mesh-like structures on matrigel culture in which expression of VM-related genes, vascular endothelial (VE)-cadherin, matrix metalloproteinase (MMP)-2 and MMP-9 was confirmed by droplet digital polymerase chain reaction (PCR). In immunofluorescence microscopy, aldehyde dehydrogenase (ALDH)1A3+ cells with properties of CSCs or progenitors and GATA binding protein 3 (GATA3)+ cells with more differentiated characteristics were localized in the bridging region and aggregated region of VM structures, respectively. In fluorescence-activated cell sorting analysis, ALDH+ cells, considered to be a subpopulation of CSCs sorted by the aldefluor assay, exhibited marked VM formation on matrigel in 24 hr, whereas ALDH− cells did not form VM, indicating possible roles of CSCs in VM formation. The stem-like cancer cells resistant to p53-induced apoptosis, which expressed a high rate of ALDH1A3 and Sex-determining region Y (SRY)-box binding protein-2 (Sox-2), completed VM formation much faster than the control. These findings may provide clues to elucidate the significance of VM formed by treatment-resistant CSCs in the metastatic potential and poor prognosis associated with TNBC.

Key words: cancer stem cell, breast cancer, vasculogenic mimicry

I. Introduction

Cancer stem cells (CSCs) are defined as having both the ability to self-renew and differentiate, and are comprised of a small population of cancer cells [27, 37, 61]. CSCs have tumor-initiating cells and are thought to be resistant to chemotherapy and radiotherapy [5, 9]. Of all the CSCs identified in solid tumors, breast CSC is one of the most commonly studied [9]. The basal-like subtype of breast cancer that is negative for estrogen receptor (ER), progesterone receptor (PR), and human epidermal growth factor receptor 2 (HER2) is referred to as triple-negative breast cancer (TNBC) [10, 24]. TNBC is also correlated with a high rate of TP53 mutations [35], and associated with a very poor prognosis and increased risk of metastasis [3, 34]. The aggressive nature of TNBC was attributed to the presence of CSCs in the cancer hierarchy [19, 31].

Evidence concerning roles of ALDH in breast cancer is accumulating whereby the metastatic and aggressive behavior of inflammatory breast cancer (IBC) is mediated by a CSC component that displays ALDH1 expression [8]. ALDH1A3, one of the subtypes of the ALDH family, was proposed as a novel clinical CSC marker showing a clear

Correspondence to: Rei Takahashi, M.D., Ph.D., Graduate School of Pharmaceutical Sciences & Faculty of Pharmaceutical Sciences, Doshisha Women's College of Liberal Arts, 97–1 Kodo, Kyotanabe, Kyoto 610–0395, Japan. E-mail: rtakahas@dwc.doshisha.ac.jp

correlation between CSC prevalence and the development of metastatic breast cancer [8, 38]. ALDH1A3 was found to be expressed in not only CSCs but also highly proliferating progenitor cells in TNBC [20]. Sox-2 (Sex-determining region Y (SRY)-box binding protein-2) plays an important role in the maintenance of the pluripotent stem cell state and regulation of embryonic development [2, 4, 44, 57, 58], and is associated with breast CSCs [26]. GATA3 (GATA binding protein 3 to DNA sequence: [A/T] GATA[A/G]) is a zinc-finger transcription factor that plays an essential role in the differentiation of breast luminal epithelium [22, 53].

Vasculogenic mimicry (VM) refers to tumor cells mimicking endothelial cells, which occurs mainly in aggressive tumors [16]. This mechanism provides tumors with a secondary circulation system of vasculogenic structures lined by tumor cells independent from angiogenesis [36]. Actual blood flow through VM in Ewing sarcoma was documented [54]. It was suggested that VM structures consisting of tumor cells might act as functional microcirculation receiving blood supply from host vessels [12, 16]. The characteristic association of expressions of VE-cadherin, MMP-2, and MMP-9 with VM formation was reported [15, 51, 55] and also documented in TNBC [31, 61].

The breast cancer cases with marked VM formation tended to be associated with a higher rate of hematogenous recurrence and a lower 5-year survival rate than non-VM cases [48]. VM formation was related to tumor invasion, metastasis, and poor prognosis [30]. TNBC-type patients show a tendency to develop visceral metastases in the early stage of their disease [7]. Patterns of recurrence were characterized by a rapidly rising rate in the first 2 years following diagnosis and a peak at 2 to 3 years, followed by a decline in recurrence risk [10, 28].

Increasing evidence suggests that CSCs are involved in VM formation in various tumor types [12]. Strong associations of VM and CSC characteristics with the aggressiveness of TNBC were also suggested [31, 61]. High levels of VM formation and ALDH1 were independently associated with metastasis and shorter overall survival (OS) in patients with epithelial ovarian carcinoma [60]. However, the occurrence and mechanisms of VM and the molecular mechanism behind the relationship between CSCs and VM formation are not fully understood.

It was reported that inhibition of VM formation via the ROS/snail signaling axis is mediated by TP53 in breast cancer [56]. The tumor suppressor gene TP53 induces cell cycle arrest and cell death after DNA damage as well as under stress-inducing conditions [21, 41]. Overexpression of p53 induces apoptosis and restricts some factors for cellular pluripotency [41, 49]. The alternative p53-mediated signaling pathways in breast CSCs lead to an apoptosis-resistant phenotype [20].

In this study, we focused on the apoptosis-resistant subpopulation of TNBC-derived HCC1937 cells with CSC characteristics, and its ability to drive VM formation on matrigel. Our results demonstrate that treatment-resistant subpopulations of TNBC cells show a significant potential for VM formation, suggesting an important role in a highly metastatic potential and poor prognosis.

II.   Materials and Methods

Construction of p53-inducible cell line and cell culture

The human breast cancer cell line HCC1937 was purchased from American Type Culture Collection (ATCC). The HCC1937 cells were negative for expressions of ER, PR, and HER2, referred to as a triple-negative tumor, and had mutations of TP53 and BRCA1 [24]. HCC1937 cells were stably transfected with a wt-p53-inducible plasmid (Tet-on Advanced System, Clontech, USA), and one of the isolated clones was designated as HCC1937/p53 and used for the experiments. The HCC1937/p53 cells were cultured in RPMI1640 (Nacalai Tesque, Kyoto, Japan), containing 10% fetal bovine serum (FBS) (SIGMA, USA) [18], and Zeocin™ (1 μg/mL, InvivoGen, USA). The HCC1937/p53 cells were cultured in doxycycline (Takara, 1 ng/mL)-containing media for 1–7 days, and those cells treated with doxycycline for 2 days were designated as Dox2d [20].

Matrigel-based in vitro VM activity assay

Matrigel® (CORNING, USA) was used. Briefly, wells of 8-well culture slides (Falcon®, CORNING, USA) were coated with 30–40 μL matrigel at 37°C for 15 min according to the thin gel method (manufacturer's protocol). The cells were suspended in opti-MEM (Life Technologies, USA) without serum and supplemented with 1% GlutaMAX™ (Life Technologies, USA) and spread on matrigel [17]. The cells were seeded on matrigel at 2.45×10^5/well. The slides were incubated in the 5% CO_2 incubator at 37°C and VM structures were observed under an inverted microscope CKX41 (OLYMPUS, Tokyo, Japan) and photographed with a DP70 digital camera (OLYMPUS, Tokyo, Japan). The photographed color image was converted to a gray-scale image using Fiji/ImageJ software (version 1.52g, Java 1.80_172, NIH) [11]. Quantitative evaluation was performed by a previously described formula (Fig. 1) for VM formation [1, 25].

Immunofluorescence

The cells on matrigel were fixed in 4% paraformaldehyde for 30 min, washed with PBS, and permeabilized with 0.25% TritonX-100 for 10 min [52]. The cells were treated with 10% normal goat serum (SeraCare Life Sciences, MA, USA) for 45 min, and incubated with primary antibodies for anti-ALDH1A3 (Purified Rabbit Polyclonal, ABGENT, 1:50), Ki-67 (Mouse IgG1 monoclonal, DAKO, 1:500), and anti-GATA3 (Mouse IgG2B monoclonal, R&D system, 1:300) at 4°C overnight. Unimmunized rabbit serum or isotype mouse IgG were used as negative controls and no background signals were observed. The specificity of these antibodies has also been widely accepted based on the manufacturer's data sheets, and publications in which specific

$$\text{VM score} = \left[\frac{(\text{No. of sprouting cells})x1 + (\text{No. of connected cells})x2 + (\text{No. of polygons})x3}{\text{Total number of cells}} \right]_{A} + \left[0, 1 \text{ or } 2 \right]_{B}$$

Fig. 1. Formula for quantification of the VM score. The VM score was assessed by a modified formula. **A**: Each cell within the optical field is counted and this number is referred to as the "total number of cells". Each cell that shows sprouting is given 1 point. When two or more prolongations unite and form connected cells, 2 points are awarded to each cell involved in this process. The formation of a polygon is given an additional 3 points. Thus, the score for sprouting, connected cells, and polygons is divided by the total number of cells. **B**: The presence of a complex mesh (luminal structures consisting of walls of two to three cells thick) is given a score of 1 and is added to the total value. This score is added once per optical field. If this complex structure is present and the walls are four or more cells thick, then a score of 2 is awarded. The absence of complex mesh receives 0 points. The individual final scores are derived from a total of ten fields each in three independent experiments.

signal bands are detected by Western blotting, and the cell type-specific immunohistochemical staining patterns have been documented [42, 46, 59]. Primary antibody binding was detected using Alexa Fluor 488 conjugated goat anti-rabbit IgG (Life Technologies, USA, 1:1,000), Alexa Fluor 680 conjugated goat anti-mouse IgG1 (γ1) (Life Technologies, USA, 1:1,000), and Alexa Fluor 680 conjugated goat anti-mouse IgG (Life Technologies, USA, 1:1,000) secondary antibodies incubated at room temperature for 1 hr. The cells were mounted and counterstained with DAPI (4,6-diamidino-2-phenylindole, dihydrochloride, 300 μg/mL) (Molecular Probes, USA) for nuclear staining. Fluorescence images were captured with a confocal laser scanning microscope (A1, NIKON INSTECH, Tokyo, Japan). Intensities of randomly selected images (total of 13 regions) were quantitatively analyzed for each fluorescence channel using Fiji/ImageJ software (version 1.52g, Java 1.80_172, NIH) [11].

ALDEFLUOR analysis and cell sorting by fluorescence-activated cell sorter (FACS)

The ALDEFLUOR kit (STEMCELL Technologies, Canada) was used to isolate the population with a high ALDH enzymatic activity [8]. HCC1937/p53 cells were suspended in the ALDEFLUOR assay buffer containing ALDH substrate (BAAA, 1 μmol/L per 1 × 10^6 cells) and incubated at 37°C for 30 min. In each experiment, a sample of cells was incubated with 50 mmol/L of the specific ALDH inhibitor diethylaminobenzaldehyde (DEAB) as a negative control. Flow cytometry sorting was conducted using a Cell Sorter SH800 (SONY, Tokyo, Japan) and SH800 Software (Ver. 2.1.2) (SONY, Tokyo, Japan). ALDEFLUOR fluorescence was excited at 488 nm wavelength and fluorescence emission was detected using a standard FITC 525/50 band pass filter (FL2). The sorting gates were established by distinguishing viable from nonviable cells using 7-aminoactinomycin D (7-AAD) (BD Biosciences, USA). The data were analyzed using SH800 Software (Ver. 2.1.2) (SONY, Tokyo, Japan).

Droplet digital PCR

The cultured cells on matrigel *en bloc* were transferred to a microcentrifuge tube. Total RNA was extracted with TRIzol® (Life Technologies, USA) and cDNA was synthesized using SuperScript® III reverse transcriptase (Life

Technologies) [11]. Droplet digital PCR (ddPCR) was performed using the QX100™ Droplet Digital™ PCR system (Bio-Rad Laboratories, Hercules, CA, USA) and according to the manufacturer's protocol. Reaction mixtures were prepared with ddPCR SuperMix (Bio-Rad Laboratories), 62.5 ng of cDNA template TaqMan® probes (Thermo Fisher Scientific, USA) for GAPDH (Hs03929097_g1), VE-cadherin (Hs00170986_m1), MMP-2 (Hs01548727_m1), and MMP-9 (Hs00957562_m1). The reaction mixture sample and Droplet Generation Oil for Probes (Bio-Rad Laboratories) were transferred to the Droplet Generator DG8 Cartridge (Bio-Rad Laboratories) and droplets were generated with QX100 ddPCR Droplet Generator (Bio-Rad Laboratories). Droplets were transferred to a 96-well PCR plate (Eppendorf, Hamburg, Germany), and the plate was then heat-sealed with pierceable foil in Heat Sealer (Eppendorf, Hamburg, Germany) and placed in C1000 Touch™ Thermo Cycler (Bio-Rad Laboratories). Conditions of thermal cycles were as follows: 95°C for 10 min, 40 cycles of 94°C for 30 sec, 60°C for 1 min followed by 98°C for 10 min (ramp rate 1°C/sec). The FAM® channel fluorescence was individually detected by QX100 ddPCR Droplet Reader (Bio-Rad Laboratories) and analyzed by QuantaSoft™ software (Ver. 1.3.2.0) (Bio-Rad Laboratories) via Poisson statistics to quantify copies per μL of reaction volume. For each sample, data were normalized to GAPDH.

Statistical analysis

All experiments were repeated at least three times. Results are expressed as Means ± SE. Differences of the values were analyzed by Student's t-test for comparison of two groups (Bell Curve for Excel Ver. 2.2.1). $P < 0.05$ was considered significant.

III. Results

VM formation of cells

The HCC1937/p53 cells exhibited various cellular sizes and pleomorphism and showed irregularly arranged aggregation without forming particular structures. The shape of individual cells was flat in a flask (Fig. 2a). On the other hand, the cells cultured on matrigel for 24 hr formed mesh-like or honeycomb structures which were similar to vascular structures (Fig. 2b). These structures are known to
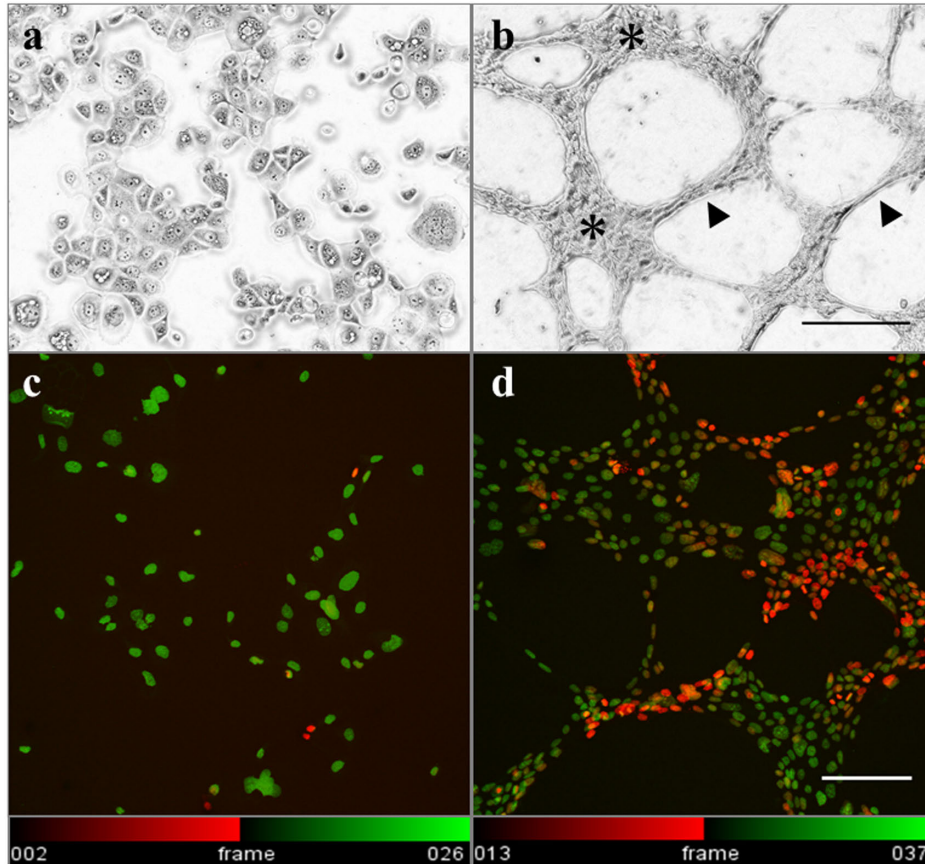
Fig. 2. VM formation of HCC1937/p53 cells on matrigel. **a) b)** Microscopic appearances of the cellular structures 24 hr after seeding on matrigel are photographed using an inverted phase contrast microscope. **a**: Cultured in flask for 24 hr. **b**: Cultured on matrigel (Bar = 200 μm). The aggregated regions (asterisks) are 4 or more cells thick, whereas the bridging regions (arrowheads) are 1–3 cells thick. **c) d)** The cells were stained with DAPI and photographed using a confocal laser scanning microscope. The 3D structures in the B regions are shown using Temporal-Color Code of Fiji/ImageJ software. Twenty-four vertical serial sections (each 1.0 μm thick) were stacked and displayed with the color code according to the depth of the nuclear location. **c**: Cells cultured on APS-coated slides for 24 hr. **d**: Cells cultured on matrigel for 24 hr (Bar = 100 μm).
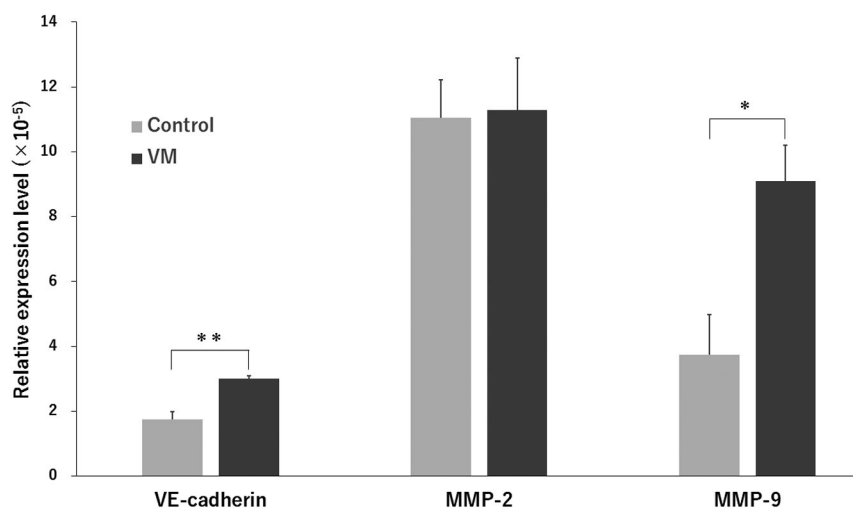

Fig. 3. Detection of VM-related gene expression in cells on matrigel by ddPCR. Control: Cells cultured in flask. VM: Cells cultured on matrigel. Relative mRNA expression level is calculated by dividing each value of the VM-related gene by that of GAPDH. Means ± SE are obtained from four independent assays for controls and five independent assays for VM experiments. **P < 0.01, *P < 0.05 (Student's t-test).
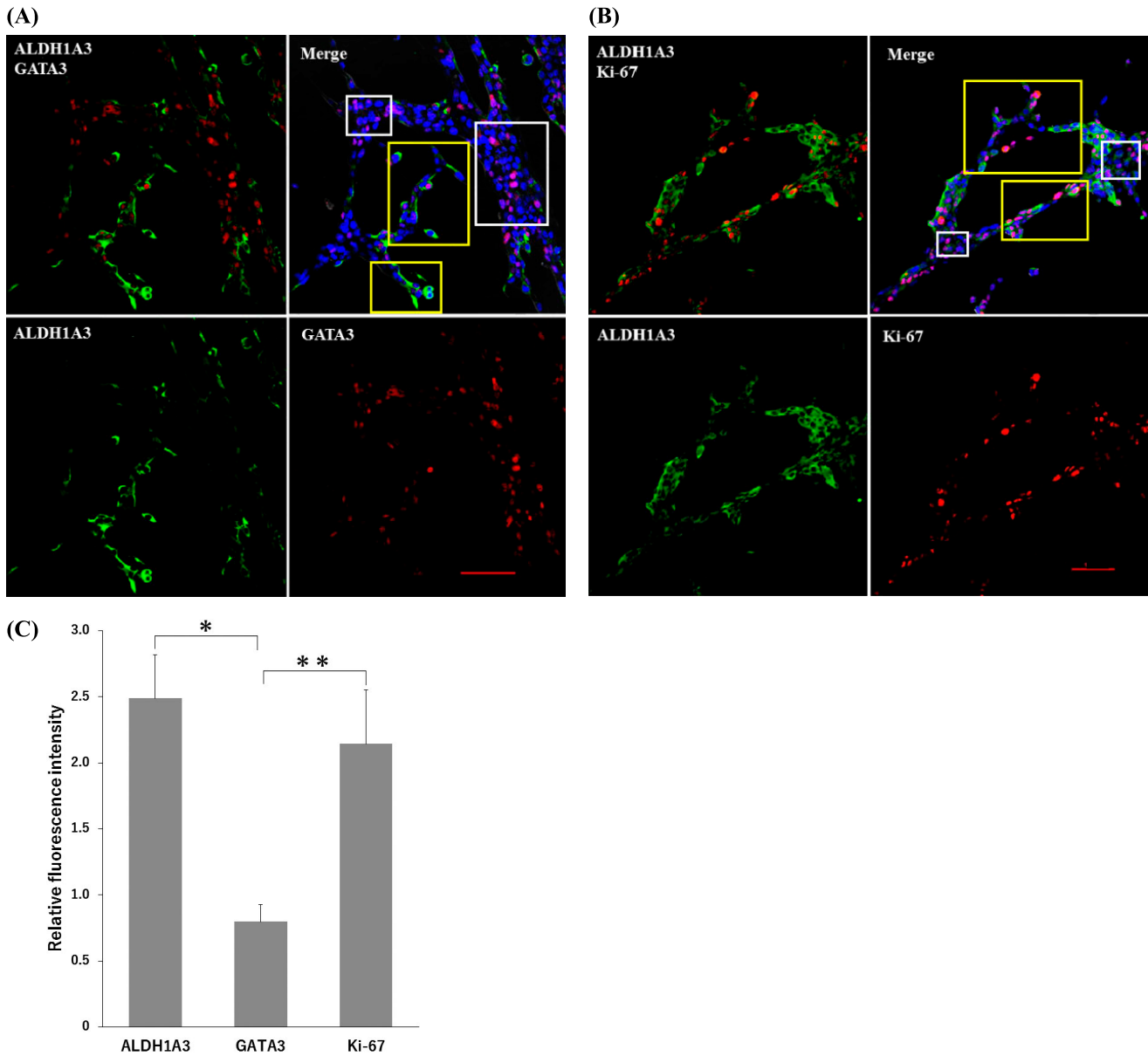
(A)

(B)

(C)

Fig. 4. Localization of gene expression patterns in the process of VM formation by double immunofluorescence analysis. Gene expression patterns in the process of VM formation. **A**: Expressions of ALDH1A3 (cytoplasm, green) and GATA3 (nuclear, read). **B**: Expressions of ALDH1A3 (cytoplasm, green) and Ki-67 (nuclear, read). Nuclei are stained with DAPI (blue). Quantitative evaluation of the expression patterns by relative fluorescence intensities. The average values of relative fluorescence intensities are obtained from the cells in yellow open squares: B region, and white open squares: A region (Bar = 100 μm). **C**: Values are obtained by dividing the total intensities by the numbers of cells in each region. Then, relative intensities (Means ± SE) are calculated as average values of the B region (n = 7) divided by those of the A region (n = 6). The experiments were repeated three times. *P < 0.05, **P < 0.05 (Student's t-test)

also be formed in breast cancer as VM. The basic structures of VM were divided into two regions. The aggregated regions (A region) are 4 or more cells thick, whereas the bridging regions (B region) are 1–3 cells thick. Interestingly, distribution analysis using Temporal-Color Code (Fiji/ImageJ) revealed three-dimensional (3D) structures in the B region (Fig. 2c and 2d). Expression levels of VM-related genes, VE-cadherin, MMP-2, and MMP-9 were then analyzed [12, 31, 55, 61] to confirm that the honeycomb structures in our experiments were formed by

the mechanisms of *bona fide* VM formation (Fig. 3). Although the expression levels of MMP-2 were almost the same between the flask control and VM, those of VE-cadherin and MMP-9 were significantly increased.

Distribution of CSCs in VM structures

The expression patterns of ALDH1A3, a breast cancer stem cell marker, and GATA3, a luminal differentiation marker, were examined in the process of VM formation by immunofluorescence microscopy. The cells that expressed
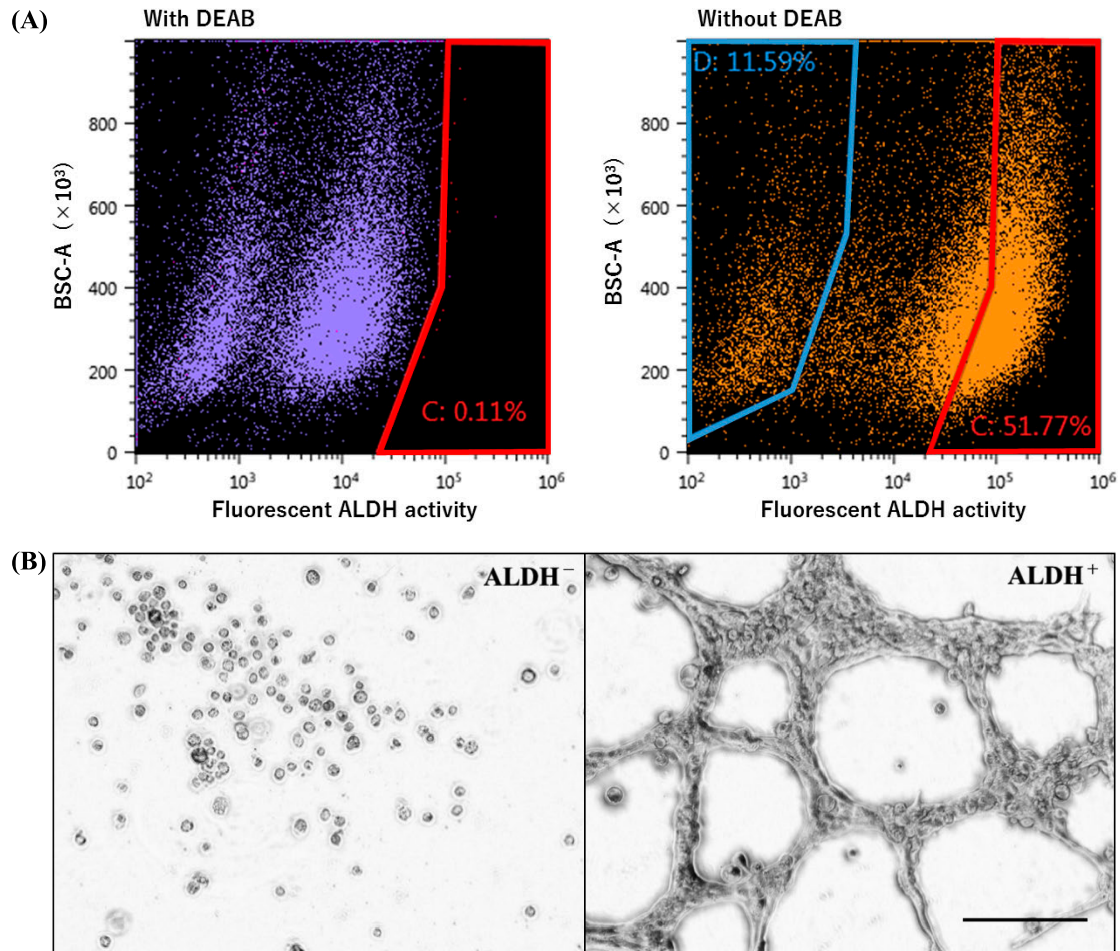
Fig. 5.   Ability of FACS-sorted ALDH+ cells to form VM. **A**: Isolation of ALDH+ and ALDH− cells by the aldefluor assay. In control, DEAB ALDH inhibitor was added to establish the baseline fluorescence of the cells (red range: 0.11%) of ALDH+ cells are defined as the cells exhibit the aldefluor activity exceeded the baseline (51.77%). ALDH− cells are defined as in the blue range, removing the intermediate range (11.59%). In order to select living cells, 7-AAD for nuclear staining was added, and the stained cells were regarded as dead cells and removed. **B**: VM formation of ALDH+ and ALDH− cells cultured on Matrigel for 24 hr (Bar = 200 μm).

ALDH1A3 tended to be localized in the B region. In contrast, the A region was characterized by expression of the ductal differentiation marker GATA3 (Fig. 4A). More proliferating cells were seen in the B region compared with the A region demonstrated by the Ki-67+ cells (Fig. 4B). To prove this preferential localization, quantitative analysis measuring the intensity of immunofluorescence was performed in each region (Fig. 4C). Statistical analysis of the relative fluorescence intensities (B region/A region) strongly suggested that the ALDH1A3+ cells and the Ki-67+ proliferating cells tended to be localized in the B region while the GATA3+ cells were in the A region (P < 0.05).

CSCs and VM formation

CSCs are known to be capable of producing vascular-like structures *in vitro* [63] and *in vivo* [43, 55]. To examine the ability of CSCs to form VM, the aldefluor assay was performed, which allowed us to detect ALDH activity and sort ALDH+ and ALDH− cells by FACS (Fig. 5A). To pre-

pare negative control samples, the ALDH inhibitor DEAB was added to establish the fluorescence baseline of the cells (red range: 0.11%). In test samples, ALDH-activated cells without DEAB treatment showed excessive fluorescence beyond the baseline increase in the number (red range: 51.77%) and were defined as ALDH+ cells. The cells with the lowest ALDH activity collected from the blue range were designated as ALDH− (blue range: 11.59%). The sorted cells were then seeded on matrigel and cultured for 24 hr (Fig. 5B). The ALDH+ cells showed conspicuous VM formation whereas ALDH− cells did not show any sprouting or aggregation, and remained round-shaped.

Apoptosis-resistant HCC1937/p53 cells and VM formation

Our previous study showed that HCC1937/p53 cells resistant to p53-induced apoptosis contain enriched CSCs, which were indicated by increased expression of the stem markers, ALDH1A3 and Sox-2 (Fig. 6). Based on the results of time-course studies, Dox2d cells were chosen
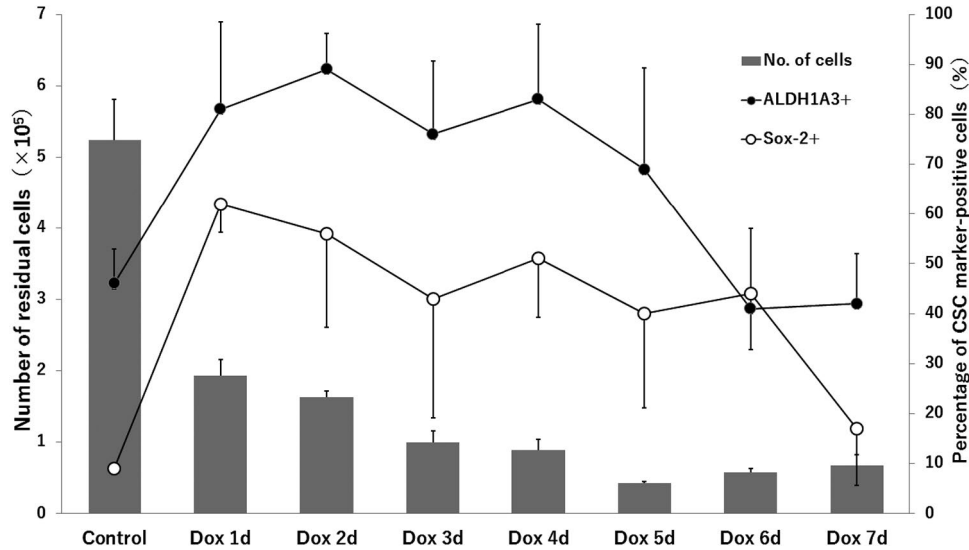
Fig. 6. The expression patterns of ALDH1A3 and Sox-2 in Dox-treated cells. The time-course changes of the percentage of ALDH1A3^{+} cells and Sox-2^{+} cells in our previous study [20] are shown. Residual HCC1937/p53 cells indicate apoptosis-resistant cells in those showing Dox-induced p53 overexpression.

because CSC-enriched populations were expected from the higher expression levels of both marker genes for CSCs. In addition before each experiment on matrigel, the induced high expression levels of ALDH1A3 and Sox-2 were reconfirmed by real-time PCR (Supplementary Fig. S1).

In control cells without doxycycline treatment, VM formation was completed in 24 hr, and then it gradually waned, probably due to the serum-free culture conditions (Fig. 7A). Dox2d cells, which were treated with doxycycline for 2 days, formed VM 6 hr earlier than the control cells, and then similarly collapsed afterwards (Fig. 7A). Actually, Dox2d cells rapidly formed VM at a higher speed than the control cells, based on linear regression analysis from 1 to 6 hr (Fig. 7B).

IV. Discussion

VM has been recognized in various types of cancer, such as breast cancer, liver cancer, glioma, ovarian cancer, melanoma, prostate cancer, and is bidirectional based on differentiated malignant tumors [60]. In an *in vivo* setting, vessel-like structures associated with malignant melanoma were devoid of endothelial cells [36], and blood flow was demonstrated in vessel-like tubes formed in Ewing sarcoma [54]. On the other hand, in *in vitro* studies, sinusoidal and tubular structures were documented by histological cross-section of cultures on matrigel involving salivary adenoid cystic carcinoma [55] and melanoma [36]. Instead of the in-gel method of matrigel culture, we chose the thin-gel culturing method, in which the three-dimensional cellular arrangement was successfully visualized by the color-coded multi-image TIFF method (Fiji/ImageJ) (Fig. 2c and 2d).

Roles of stem-like cancer cells in induction of VM were suggested in various cancer types. For example, stem-like cancer cells were identified and isolated by ALDH activity [25], by the ability of mammosphere formation [32], and by expressions of CD133 [31, 55], CD44^{+}/CD24^{−} [25, 39], and Sox-2 [26]. In inflammatory breast cancer (IBC) with a poor prognosis, invasion and metastasis were mediated by subpopulations of cells that exhibited ALDH activity [8], and correlated with a high rate of VM formation [48]. In a xenograft tumor of IBC, a VM-angiogenesis junction was identified, suggesting the possible role of VM in metastasis [47]. The HCC1937 cells we used were derived from basal-like breast cancer [24] showing a higher ratio of ALDH[+] CSCs [6, 19, 20]. The conspicuous ability of FACS-sorted ALDH^{+} cells to form VM was previously documented in breast cancer cells [25], which is consistent with the consensus that VM is a marker of a poor prognosis associated with malignancies [60]. In this study, we demonstrated that the ALDH^{+} cells were capable of forming VM in 24 hr while the ALDH^{−} cells lacked this ability. These results clearly indicate that the cells with the property of CSCs in ALDH[+] subpopulations are essential for their ability to form VM.

Immunofluorescence analysis on matrigel revealed the preferential localization of ALDH1A3^{+} cells in the VM-forming B regions, suggesting possible roles of CSCs in proceeding VM. According to our previous study, activation of CSCs with ALDH1A3 overexpression was followed by cell proliferation with Ki-67 expression, and further cell differentiation with GATA3 expression [20]. Therefore, activated CSCs first started cell proliferation with Ki-67 expression in the B region and further differentiated to GATA3^{+} cells in the A region, which resulted in VM formation. Although GATA3 is a marker of mammary ductal morphogenesis, modulation of its expression was also verified in vasculogenesis and angiogenesis of human embry-
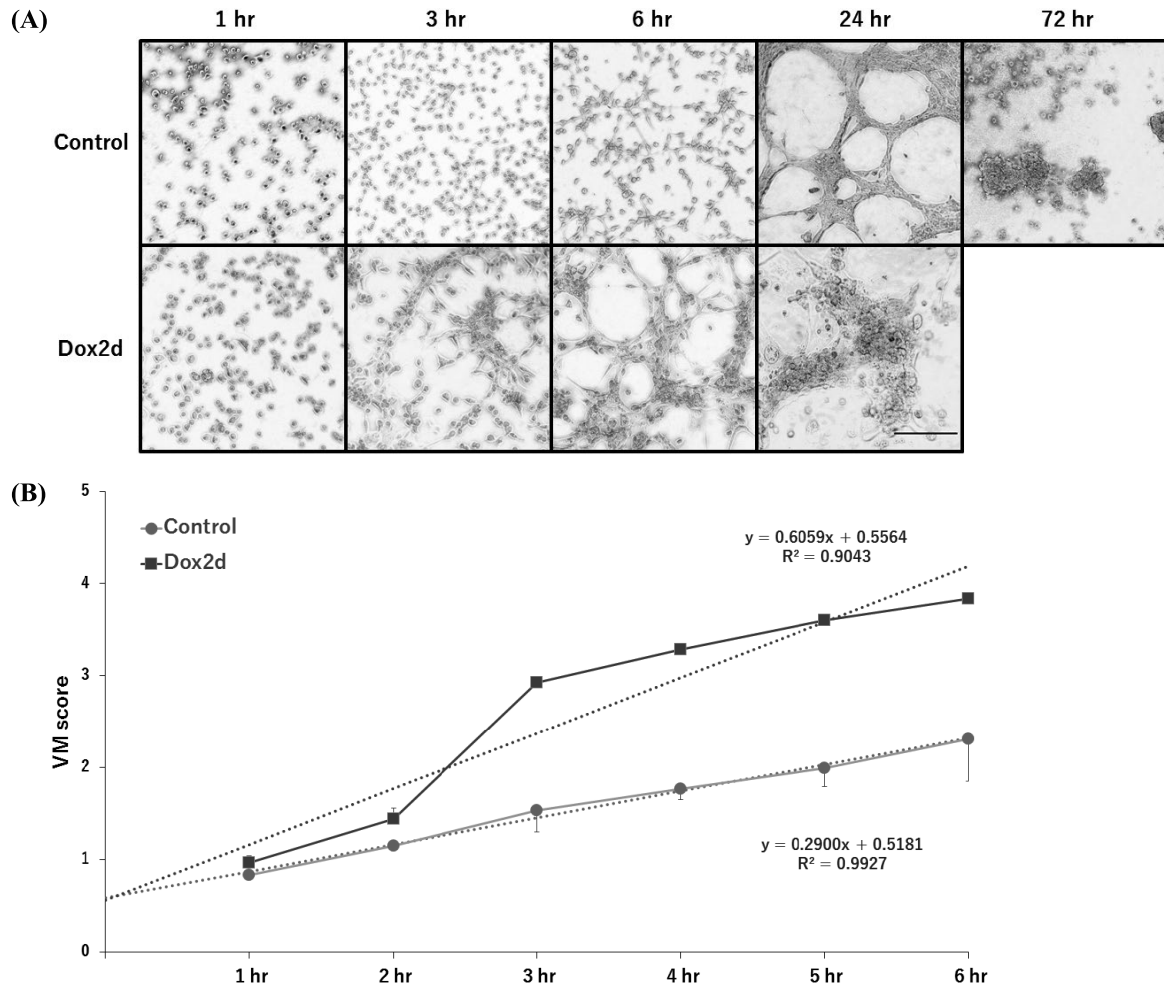
(A)

(B)

Fig. 7.   Accelerated VM formation on matrigel in apoptosis-resistant subpopulations of HCC1937/p53 cells. **A**: The cells on doxycycline for 2 days were seeded in matrigel and cultured. The control cells were not treated with doxycycline. **B**: The time-course changes of VM scores were calculated by the formula in Fig. 1. Each line graph is modified by linear regression (Control: $R^2 = 0.9927$, Dox2d: $R^2 = 0.9043$) and shown as a dotted line.

onic stem cells [13], and essential for the activation of human endothelial cells [50]. Thus, our results suggest the critical role of CSCs in the initiation of VM formation.

   There may be several reasons why the Dox2d cells exhibited more rapid VM formation compared with FACS-sorted ALDH⁺ cells. First, the rate of p53-resistant cells on Dox2d was 31.05% of the total HCC1937/p53 cells (Fig. 6), while 51.77% of ALDH⁺ cells isolated by FACS were used (Fig. 5A). Therefore, Dox2d cells used for the VM-forming assay would have contained more CSCs capable of VM formation. Second, VM occurs under some stressed conditions when the tumor environment is hypoxic or tumor cells require an increased blood supply [23, 29], resulting in further transformation to a more aggressive cancer phenotype. Similarly, the cells under the stress of p53-induced apoptosis may acquire the ability to form VM if they are able to survive. Downregulation of VM formation induced by enhanced expression of the p53 gene was reported, suggesting a possible relationship between VM formation and p53 overexpression [56]. The Dox2d cells in

our experiments showed a strong VM-forming capability, probably because some mechanism for generating p53 resistance may have restored the ability to form VM. In fact, p53-resistant Dox2d cells expressed not only significant amounts of ALDH1A3, Sox-2, and GATA3, but also expressed VM-related factors, including VE-cadherin and MMP9 (Supplementary Fig. S2).

   Vasculogenic mimicry refers to the ability of some malignant cells to start a dedifferentiation process to adopt multiple cellular phenotypes, including endothelial-like properties [36, 64]. The reactivation of stem cell-associated markers or pluripotency factors may cause dedifferentiation and a more stem cell-like state. Epithelial-mesenchymal transition (EMT) is one of the dedifferentiation processes that plays an integral role in tumor progression [40]. Sox-2 regulates self-renewal and maintenance in cancer stem cell populations in various cancer types [14]. In fact, expression of Sox-2 was upregulated in the presence of VM formation according to our data (Supplementary Fig. S3).

   TNBC is known to be a poor prognostic and drug-

resistant tumor because it may contain more CSCs than other types of breast cancer [7, 10]. As one of the mechanisms for these characteristics, the occurrence of VM formation in TNBC has been proposed [31, 61, 62]. In our experiments, the TNBC-derived HCC1937/p53 cells rescued from p53-induced apoptosis exhibited stem-like properties and accelerated VM formation. This is the first direct evidence that treatment-resistant subpopulations in TNBC play important roles in VM formation. Anti-VM formation therapy would be an alternative method to block blood supply to tumor cells when anti-angiogenesis therapy is ineffective.

V. Conflicts of Interest

VI. Acknowledgments

VII. References

1. Aranda, E. and Owen, G. I. (2009) A semi-quantitative assay to screen for angiogenic compounds and compounds with angiogenic potential using the EA.hy926 endothelial cell line. *Biol. Res.* 42; 377–389.
2. Avilion, A. A., Nicolis, S. K., Pevny, L. H., Perez, L., Vivian, N. and Lovell-Badge, R. (2003) Multipotent cell lineages in early mouse development depend on SOX2 function. *Genes Dev.* 17; 126–140.
3. Barcellos-Hoff, M. H. and Kleinberg, D. L. (2013) Breast cancer risk in BRCA1 mutation carriers: insight from mouse models. *Ann. Oncol.* 24; viii8–viii12.
4. Batchuluun, K., Azuma, M., Fujiwara, K., Yashiro, T. and Kikuchi, M. (2017) Notch signaling and maintenance of SOX2 expression in rat anterior pituitary cells. *Acta Histochem. Cytochem.* 50; 63–69.
5. Bomken, S., Fišer, K., Heidenreich, O. and Vormoor, J. (2010) Understanding the cancer stem cell. *Br. J. Cancer* 103; 439–445.
6. Burga, L. N., Tung, N. M., Troyan, S. L., Bostina, M., Konstantinopoulos, P. A., Fountzilas, H., Spentzos, D., Miron, A., Yassin, Y. A., Lee, B. T. and Wulf, G. M. (2009) Altered proliferation and differentiation properties of primary mammary epithelial cells from BRCA1 mutation carriers. *Cancer Res.* 69; 1273–1278.
7. Carey, L. A., Dees, E. C., Sawyer, L., Gatti, L., Moore, D. T., Collichio, F., Ollila, D. W., Sartor, C. I., Graham, M. L. and Perou, C. M. (2007) The triple negative paradox: primary tumor chemosensitivity of breast cancer subtypes. *Clin. Cancer Res.* 13; 2329–2334.
8. Charafe-Jauffret, E., Ginestier, C., Iovino, F., Tarpin, C., Diebel, M., Esterni, B., Houvenaeghel, G., Extra, J.-M., Bertucci, F., Jacquemier, J., Xerri, L., Dontu, G., Stassi, G., Xiao, Y., Barsky, S. H., Birnbaum, D., Viens, P. and Wicha, M. S. (2010) Aldehyde dehydrogenase 1-positive cancer stem cells mediate metastasis and poor clinical outcome in inflammatory breast cancer. *Clin. Cancer Res.* 16; 45–55.
9. Chuthapisith, S., Eremin, J., El-Sheemey, M. and Eremin, O. (2010) Breast cancer chemoresistance: Emerging importance of cancer stem cells. *Surg. Oncol.* 19; 27–32.
10. Dent, R., Trudeau, M., Pritchard, K. I., Hanna, W. M., Kahn, H. K., Sawka, C. A., Lickley, L. A., Rawlinson, E., Sun, P. and Narod, S. A. (2007) Triple-negative breast cancer: clinical features and patterns of recurrence. *Clin. Cancer Res.* 13; 4429–4434.
11. Egashira, N., Minematsu, T., Miyai, S., Takekoshi, S., Camper, S. A. and Osamura, R. Y. (2008) Pituitary changes in Prop1 transgenic mice: hormone producing tumors and signet-ring type gonadotropes. *Acta Histochem. Cytochem.* 41; 47–57.
12. Fan, Y.-L., Zheng, M., Tang, Y.-L. and Liang, X.-H. (2013) A new perspective of vasculogenic mimicry: EMT and cancer stem cells (Review). *Oncol. Lett.* 6; 1174–1180.
13. Gerecht-Nir, S., Dazard, J.-E., Golan-Mashiach, M., Osenberg, S., Botvinnik, A., Amariglio, N., Domany, E., Rechavi, G., Givol, D. and Itskovitz-Eldor, J. (2005) Vascular gene expression and phenotypic correlation during differentiation of human embryonic stem cells. *Dev. Dyn.* 232; 487–497.
14. Herreros-Villanueva, M., Zhang, J.-S., Koenig, A., Abel, E. V., Smyrk, T. C., Bamlet, W. R., de Narvajas, A. A.-M., Gomez, T. S., Simeone, D. M., Bujanda, L. and Billadeau, D. D. (2013) SOX2 promotes dedifferentiation and imparts stem cell-like features to pancreatic cancer cells. *Oncogenesis* 2; e61.
15. Hess, A. R., Seftor, E. A., Seftor, R. E. B. and Hendrix, M. J. C. (2003) Phosphoinositide 3-kinase regulates membrane Type 1-matrix metalloproteinase (MMP) and MMP-2 activity during melanoma cell vasculogenic mimicry. *Cancer Res.* 63; 4757–4762.
16. Hillen, F. and Griffioen, A. W. (2007) Tumour vascularization: sprouting angiogenesis and beyond. *Cancer Metastasis Rev.* 26; 489–502.
17. Hongisto, V., Jernström, S., Fey, V., Mpindi, J.-P., Kleivi Sahlberg, K., Kallioniemi, O. and Perälä, M. (2013) High-throughput 3D screening reveals differences in drug sensitivities between culture models of JIMT1 breast cancer cells. *PLoS One* 8; e77232.
18. Iwabuchi, E., Miki, Y., Ono, K., Onodera, Y. and Sasano, H. (2017) In situ evaluation of estrogen receptor dimers in breast carcinoma cells: visualization of protein-protein interactions. *Acta Histochem. Cytochem.* 50; 85–93.
19. Kai, M., Kanaya, N., Wu, S. V., Mendez, C., Nguyen, D., Luu, T. and Chen, S. (2015) Targeting breast cancer stem cells in triple-negative breast cancer using a combination of LBH589 and salinomycin. *Breast Cancer Res. Treat.* 151; 281–294.
20. Kashii-Magaribuchi, K., Takeuchi, R., Haisa, Y., Sakamoto, A., Itoh, A., Izawa, Y., Isa, M., Fukuzawa, M., Murakami, M. and Takahashi, R. (2016) Induced expression of cancer stem cell markers ALDH1A3 and Sox-2 in hierarchical reconstitution of apoptosis-resistant human breast cancer cells. *Acta Histochem. Cytochem.* 49; 149–158.
21. Ko, L. J. and Prives, C. (1996) p53: puzzle and paradigm. *Genes Dev.* 10; 1054–1072.
22. Kouros-Mehr, H., Bechis, S. K., Slorach, E. M., Littlepage, L. E., Egeblad, M., Ewald, A. J., Pai, S., Ho, I. and Werb, Z. (2008) GATA-3 links tumor differentiation and dissemination in a luminal breast cancer model. *Cancer Cell* 13; 141–152.
23. Larson, A. R., Lee, C.-W., Lezcano, C., Zhan, Q., Huang, J., Fischer, A. H. and Murphy, G. F. (2014) Melanoma spheroid formation involves laminin-associated vasculogenic mimicry. *Am. J. Pathol.* 184; 71–78.
24. Lawrence, R. T., Perez, E. M., Hernández, D., Miller, C. P., Haas, K. M., Irie, H. Y., Lee, S.-I., Blau, C. A. and Villén, J.

(2015) The proteomic landscape of triple-negative breast cancer. *Cell Rep.* 11; 630–644.

25. Lee, C.-H., Wu, Y.-T., Hsieh, H.-C., Yu, Y., Yu, A. L. and Chang, W.-W. (2014) Epidermal growth factor/heat shock protein 27 pathway regulates vasculogenic mimicry activity of breast cancer stem/progenitor cells. *Biochimie* 104; 117–126.

26. Leis, O., Eguiara, A., Lopez-Arribillaga, E., Alberdi, M. J., Hernandez-Garcia, S., Elorriaga, K., Pandiella, A., Rezola, R. and Martin, A. G. (2012) Sox2 expression in breast tumours and activation in breast cancer stem cells. *Oncogene* 31; 1354–1365.

27. Li, X., Xu, Y., Chen, Y., Chen, S., Jia, X., Sun, T., Liu, Y., Li, X., Xiang, R. and Li, N. (2013) SOX2 promotes tumor metastasis by stimulating epithelial-to-mesenchymal transition via regulation of WNT/β-catenin signal network. *Cancer Lett.* 336; 379–389.

28. Liedtke, C., Mazouni, C., Hess, K. R., André, F., Tordai, A., Mejia, J. A., Symmans, W. F., Gonzalez-Angulo, A. M., Hennessy, B., Green, M., Cristofanilli, M., Hortobagyi, G. N. and Pusztai, L. (2008) Response to neoadjuvant therapy and long-term survival in patients with triple-negative breast cancer. *J. Clin. Oncol.* 26; 1275–1281.

29. Liu, K., Sun, B., Zhao, X., Wang, X., Li, Y., Qiu, Z., Liu, T., Gu, Q., Dong, X., Zhang, Y., Wang, Y. and Zhao, N. (2015) Hypoxia promotes vasculogenic mimicry formation by the Twist1-Bmi1 connection in hepatocellular carcinoma. *Int. J. Mol. Med.* 36; 783–791.

30. Liu, T., Sun, B., Zhao, X., Li, Y., Zhao, X., Liu, Y., Yao, Z., Gu, Q., Dong, X., Shao, B., Lin, X., Liu, F. and An, J. (2015) USP44+ cancer stem cell subclones contribute to breast cancer aggressiveness by promoting vasculogenic mimicry. *Mol. Cancer Ther.* 14; 2121–2131.

31. Liu, T. J., Sun, B. C., Zhao, X. L., Zhao, X. M., Sun, T., Gu, Q., Yao, Z., Dong, X. Y., Zhao, N. and Liu, N. (2013) CD133+ cells with cancer stem cell characteristics associates with vasculogenic mimicry in triple-negative breast cancer. *Oncogene* 32; 544–553.

32. Liu, Y., Sun, B., Liu, T., Zhao, X., Wang, X., Li, Y., Meng, J., Gu, Q., Liu, F., Dong, X., Liu, P., Sun, R. and Zhao, N. (2016) Function of AURKA protein kinase in the formation of vasculogenic mimicry in triple-negative breast cancer stem cells. *Onco Targets Ther.* 9; 3473–3484.

33. Livak, K. J. and Schmittgen, T. D. (2001) Analysis of relative gene expression data using real-time quantitative PCR and the 2-ΔΔCT method. *Methods* 25; 402–408.

34. Livasy, C. A., Karaca, G., Nanda, R., Tretiakova, M. S., Olopade, O. I., Moore, D. T. and Perou, C. M. (2006) Phenotypic evaluation of the basal-like subtype of invasive breast carcinoma. *Mod. Pathol.* 19; 264–271.

35. Manié, E., Vincent-Salomon, A., Lehmann-Che, J., Pierron, G., Turpin, E., Warcoin, M., Gruel, N., Lebigot, I., Sastre-Garau, X., Lidereau, R., Remenieras, A., Feunteun, J., Delattre, O., De Thé, H., Stoppa-Lyonnet, D. and Stern, M. H. (2009) High frequency of TP53 mutation in BRCA1 and sporadic basal-like carcinomas but not in BRCA1 luminal breast tumors. *Cancer Res.* 69; 663–671.

36. Maniotis, A. J., Folberg, R., Hess, A., Seftor, E. A., Gardner, L. M. G., Pe'er, J., Trent, J. M., Meltzer, P. S. and Hendrix, M. J. C. (1999) Vascular channel formation by human melanoma cells in vivo and in vitro: vasculogenic mimicry. *Am. J. Pathol.* 155; 739–752.

37. Marcato, P., Dean, C. A., Giacomantonio, C. A. and Lee, P. W. K. (2011) Aldehyde dehydrogenase its role as a cancer stem cell marker comes down to the specific isoform. *Cell Cycle* 10; 1378–1384.

38. Marcato, P., Dean, C. A., Pan, D., Araslanova, R., Gillis, M., Joshi, M., Helyer, L., Pan, L., Leidal, A., Gujar, S., Giacomantonio, C. A. and Lee, P. W. K. (2011) Aldehyde dehydrogenase activity of breast cancer stem cells is primarily due to isoform ALDH1A3 and its expression is predictive of metastasis. *Stem Cells* 29; 32–45.

39. Paulis, Y. W. J., Huijbers, E. J. M., van der Schaft, D. W. J., Soetekouw, P. M. M. B., Pauwels, P., Tjan-Heijnen, V. C. G. and Griffioen, A. W. (2015) CD44 enhances tumor aggressiveness by promoting tumor cell plasticity. *Oncotarget* 6; 19634–19646.

40. Qiao, L., Liang, N., Zhang, J., Xie, J., Liu, F., Xu, D., Yu, X. and Tian, Y. (2015) Advanced research on vasculogenic mimicry in cancer. *J. Cell. Mol. Med.* 19; 315–326.

41. Qin, H., Yu, T., Qing, T., Liu, Y., Zhao, Y., Cai, J., Li, J., Song, Z., Qu, X., Zhou, P., Wu, J., Ding, M. and Deng, H. (2007) Regulation of apoptosis and differentiation by p53 in human embryonic stem cells. *J. Biol. Chem.* 282; 5842–5852.

42. Rexer, B. N., Zheng, W. L. and Ong, D. E. (2001) Retinoic acid biosynthesis by normal human breast epithelium is via aldehyde dehydrogenase 6, absent in MCF-7 cells. *Cancer Res.* 61; 7065–7070.

43. Ricci-Vitiani, L., Pallini, R., Biffoni, M., Todaro, M., Invernici, G., Cenci, T., Maira, G., Parati, E. A., Stassi, G., Larocca, L. M. and De Maria, R. (2010) Tumour vascularization via endothelial differentiation of glioblastoma stem-like cells. *Nature* 468; 824–830.

44. Sarkar, A. and Hochedlinger, K. (2013) The Sox family of transcription factors: Versatile regulators of stem and progenitor cell fate. *Cell Stem Cell* 12; 15–30.

45. Schmittgen, T. D. and Livak, K. J. (2008) Analyzing real-time PCR data by the comparative CT method. *Nat. Protoc.* 3; 1101–1108.

46. Shi, S. R., Key, M. E. and Kalra, K. L. (1991) Antigen retrieval in formalin-fixed, paraffin-embedded tissues: an enhancement method for immunohistochemical staining based on microwave oven heating of tissue sections. *J. Histochem. Cytochem.* 39; 741–748.

47. Shirakawa, K., Kobayashi, H., Heike, Y., Iwanaga, T., Konishi, F., Terada, M. and Wakasugi, H. (2002) Hemodynamics in vasculogenic mimicry and angiogenesis of inflammatory breast cancer xenograft hemodynamics in vasculogenic mimicry and angiogenesis of inflammatory breast. *Cancer Res.* 2; 560–566.

48. Shirakawa, K., Wakasugi, H., Heike, Y., Watanabe, I., Yamada, S., Saito, K. and Konishi, F. (2002) Vasculogenic mimicry and pseudo-comedo formation in breast cancer. *Int. J. Cancer* 99; 821–828.

49. Solozobova, V. and Blattner, C. (2011) p53 in stem cells. *World J. Biol. Chem.* 2; 202–214.

50. Song, H., Suehiro, J. I., Kanki, Y., Kawai, Y., Inoue, K., Daida, H., Yano, K., Ohhashi, T., Oettgen, P., Aird, W. C., Kodama, T. and Minami, T. (2009) Critical role for GATA3 in mediating Tie2 expression and function in large vessel endothelial cells. *J. Biol. Chem.* 284; 29109–29124.

51. Sun, T., Zhao, N., Zhao, X., Gu, Q., Zhang, S., Che, N., Wang, X., Du, J., Liu, Y. and Sun, B. (2010) Expression and functional significance of Twist1 in hepatocellular carcinoma: Its role in vasculogenic mimicry. *Hepatology* 51; 545–556.

52. Syaidah, R., Tsukada, T., Azuma, M., Horiguchi, K., Fujiwara, K., Kikuchi, M. and Yashiro, T. (2016) Fibromodulin expression in folliculostellate cells and pericytes is promoted by TGFβ signaling in rat anterior pituitary gland. *Acta Histochem. Cytochem.* 49; 171–179.

53. Takaku, M., Grimm, S. A. and Wade, P. A. (2015) GATA3 in breast cancer: tumor suppressor or oncogene? *Gene Expr.* 16; 163–168.

54. Van Der Schaft, D. W. J., Hillen, F., Pauwels, P., Kirschmann, D. A., Castermans, K., Oude Egbrink, M. G. A., Tran, M. G. B., Sciot, R., Hauben, E., Hogendoorn, P. C. W., Delattre, O.,

Maxwell, P. H., Hendrix, M. J. C. and Griffioen, A. W. (2005) Tumor cell plasticity in Ewing sarcoma, an alternative circulatory system stimulated by hypoxia. *Cancer Res.* 65; 11520–11528.

55. Wang, S., Gao, X., Liu, X., Gao, S., Fan, Y., Jiang, Y., Ma, X., Jiang, J., Feng, H., Chen, Q., Tang, Y., Tang, Y. and Liang, X. (2016) CD133+ cancer stem-like cells promote migration and invasion of salivary adenoid cystic carcinoma by inducing vasculogenic mimicry formation. *Oncotarget* 7; 29051–29062.

56. Wang, Y., Sun, H., Zhang, D., Fan, D., Zhang, Y., Dong, X., Liu, S., Yang, Z., Ni, C., Li, Y., Liu, F. and Zhao, X. (2018) TP53INP1 inhibits hypoxia-induced vasculogenic mimicry formation via the ROS/snail signalling axis in breast cancer. *J. Cell. Mol. Med.* 22; 3475–3488.

57. Weina, K. and Utikal, J. (2014) SOX2 and cancer: current research and its implications in the clinic. *Clin. Transl. Med.* 3; 1–10.

58. Yamanaka, S. (2007) Strategies and new developments in the generation of patient-specific pluripotent stem cells. *Cell Stem Cell* 1; 39–49.

59. Yoshida, A., Rzhetsky, A., Hsu, L. C. and Chang, C. (1998) Human aldehyde dehydrogenase gene family. *Eur. J. Biochem.* 251; 549–557.

60. Yu, L., Zhu, B., Wu, S., Zhou, L., Song, W., Gong, X. and Wang, D. (2017) Evaluation of the correlation of vasculogenic mimicry, ALDH1, KiSS-1, and MACC1 in the prediction of metastasis and prognosis in ovarian carcinoma. *Diagn. Pathol.* 12; 23.

61. Zeng, F., Ju, R., Liu, L., Xie, H., Mu, L., Zhao, Y., Yan, Y., Hu, Y.-J., Wu, J.-S. and Lu, W.-L. (2015) Application of functional vincristine plus dasatinib liposomes to deletion of vasculogenic mimicry channels in triple-negative breast cancer. *Oncotarget* 6; 36625–36642.

62. Zhang, D., Sun, B., Zhao, X., Ma, Y., Ji, R., Gu, Q., Dong, X., Li, J., Liu, F., Jia, X., Leng, X., Zhang, C., Sun, R. and Chi, J. (2014) Twist1 expression induced by sunitinib accelerates tumor cell vasculogenic mimicry by increasing the population of CD133+cells in triple-negative breast cancer. *Mol. Cancer* 13; 1–14.

63. Zhang, J., Qiao, L., Liang, N., Xie, J., Luo, H., Deng, G. and Zhang, J. (2016) Vasculogenic mimicry and tumor metastasis. *J. BUON.* 21; 533–541.

64. Zuazo-Gaztelu, I. and Casanovas, O. (2018) Unraveling the role of angiogenesis in cancer ecosystems. *Front. Oncol.* 8; 248.